6

Passivity-Based Control and Sliding Mode Control applied to Electric Vehicles based on Fuel Cells, Supercapacitors and Batteries on the DC Link

M. Becherif[1,2], M. Y. Ayad[1], A. Henni[3], M. Wack[1], A. Aboubou[4], A. Allag[4] and M. Sebaï[4]
[1] *SeT Laboratory, UTBM University, France*
[2] *FC-Lab fuel Cell Laboratory, UTBM University, France*
[3] *Alstom Power System, Energy Management Business, France*
[4] *LMSE Laboratory, Biskra University, Algeria*

1. Introduction

Fuel Cells (FC) produce electrical energy from an electrochemical reaction between a hydrogen-rich fuel gas and an oxidant (air or oxygen) (Kishinevsky & Zelingher, 2003) (Larminie & Dicks, 2000). They are high-current, and low-voltage sources. Their use in embedded systems becomes more interesting when using storage energy elements, like batteries, with high specific energy, and supercapacitors (SC), with high specific power. In embedded systems, the permanent source which can either be FC's or batteries must produce the limited permanent energy to ensure the system autonomy (Pischinger et al., 2006) (Moore et al., 2006) (Corrêa et al., 2003). In the transient phase, the storage devices produce the lacking power (to compensate for deficit in power required) in acceleration function, and absorbs excess power in braking function. FC's, and due to its auxiliaries, have a large time constant (several seconds) to respond to an increase or decrease in power output. The SCs are sized for the peak load requirements and are used for short duration load levelling events such as fuel starting, acceleration and braking (Rufer et al, 2004) (Thounthong et al., 2007). These short durations, events are experienced thousands of times throughout the life of the hybrid source, require relatively little energy but substantial power (Granovskii et al.,2006) (Benziger et al., 2006).
Three operating modes are defined in order to manage energy exchanges between the different power sources. In the first mode, the main source supplies energy to the storage device. In the second mode, the primary and secondary sources are required to supply energy to the load. In the third, the load supplies energy to the storage device.
In this work, we present a new concept of a hybrid DC power source using SC's as auxiliary storage device, a Proton Exchange Membrane Fuel Cell (PEMFC) as the main energy source. The source is also composed of batteries on a DC link. The general structure of the studied system is presented and a dynamic model of the overall system is given. Two control

techniques are presented. The first is based on passivity based control (PBC) (Ortega et al. 2002). The system is written in a Port Controlled Hamiltonian (PCH) form where important structural properties are exhibited (Becherif et al., 2005). Then a PBC of the system is presented which proves the global stability of the equilibrium with the proposed control laws. The second is based on nonlinear sliding mode control for the DC-DC supercapacitors converter and a linear regulation for the FC converter (Ayad et al. 2007). Finally, simulation results using Matlab are given

2. State of the art and potential application

2.1. Fuel Cells

A. Principle

The developments leading to an operational FC can be traced back to the early 1800's with Sir William Grove recognized as the discoverer in 1839.

A FC is an energy conversion device that converts the chemical energy of a fuel directly into electricity. Energy is released whenever a fuel (hydrogen) reacts chemically with the oxygen of air. The reaction occurs electrochemically and the energy is released as a combination of low-voltage DC electrical energy and heat.

Types of FCs differ principally by the type of electrolyte they utilize (Fig. 1). The type of electrolyte, which is a substance that conducts ions, determines the operating temperature, which varies widely between types.

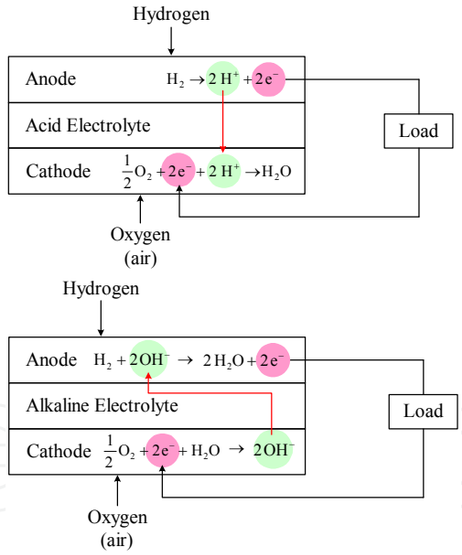

Fig. 1. Principle of acid (top) and alkaline (bottom) electrolytes fuel cells

Proton Exchange Membrane (or "solid polymer") Fuel Cells (PEMFCs) are presently the most promising type of FCs for automotive use and have been used in the majority of prototypes built to date.

The structure of a cell is represented in Fig. 2. The gases flowing along the x direction come from channels designed in the bipolar plates (thickness 1-10 mm). Vapour water is added to the gases to humidify the membrane. The diffusion layers (100-500 µm) ensure a good distribution of the gases to the reaction layers (5-50 µm). These layers constitute the

electrodes of the cell made of platinum particles, which play the role of catalyst, deposited within a carbon support on the membrane.

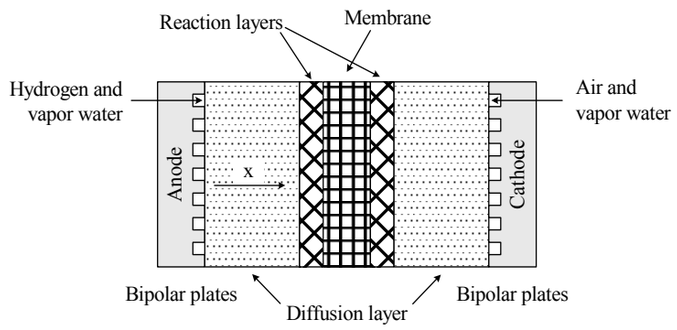

Fig. 2. Different layers of an elementary cell

Hydrogen oxidation and oxygen reduction:

$$\begin{aligned} H_2 &\rightarrow 2H^+ + 2e^- \quad \text{anode} \\ 2H^+ + 2e^- + \frac{1}{2}O_2 &\rightarrow H_2O \quad \text{cathode} \end{aligned} \tag{1}$$

The two electrodes are separated by the membrane (20-200 µm) which carries protons from the anode to the cathode and is impermeable to electrons. This flow of protons drags water molecules as a gradient of humidity leads to the diffusion of water according to the local humidity of the membrane. Water molecules can then go in both directions inside the membrane according to the side where the gases are humidified and to the current density which is directly linked to the proton flow through the membrane and to the water produced on the cathode side.
Electrons which appear on the anode side cannot cross the membrane and are used in the external circuit before returning to the cathode. Proton flow is directly linked to the current density:

$$J_{H^+} = \frac{i}{F} \tag{2}$$

where F is the Faraday's constant.
The value of the output voltage of the cell is given by Gibb's free energy ΔG and is:

$$V_{rev} = -\frac{\Delta G}{2.F} \tag{3}$$

This theoretical value is never reached, even at no load condition. For the rated current (around 0.5 A.cm^{-2}), the voltage of an elementary cell is about 0.6-0.7 V.
As the gases are supplied in excess to ensure a good operating of the cell, the non-consumed gases have to leave the FC, carrying with them the produced water.

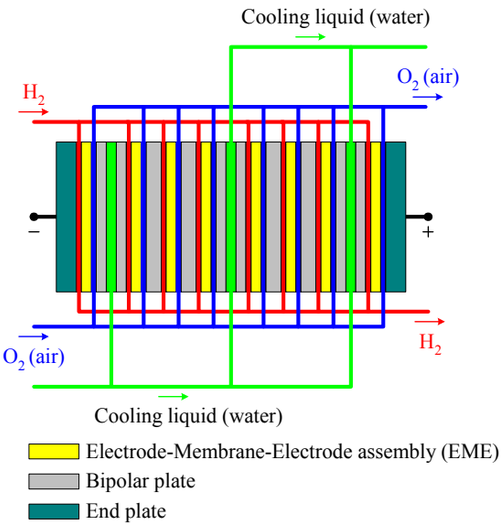

Fig. 3. External and internal connections of a PEMFC stack

Generally, a water circuit is used to impose the operating temperature of the FC (around 60-70 °C). At start up, the FC is warmed and later cooled as at the rated current nearly the same amount of energy is produced under heat form than under electrical form.

B. Modeling Fuel Cell

The output voltage of a single cell V_{FC} can be defined as the result of the following static and nonlinear expression (Larminie & Dicks, 2000):

$$V_{FC} = E - V_{act} - V_{ohm} - V_{concent} \tag{4}$$

where *E* is the thermodynamic potential of the cell and it represents its reversible voltage, V_{act} is the voltage drop due to the activation of the anode and of the cathode, V_{ohm} is the ohmic voltage drop, a measure of the ohmic voltage drop associated with the conduction of the protons through the solid electrolyte and electrons through the internal electronic resistances, and $V_{concent}$ represents the voltage drop resulting from the concentration or mass transportation of the reacting gases.

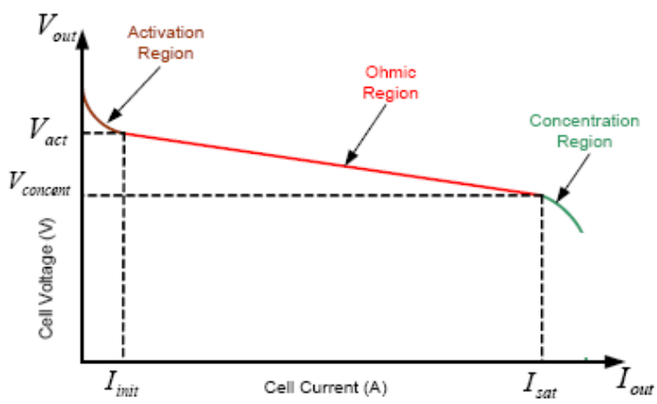

Fig. 4. A typical polarization curve for a PEMFC

In (4), the first term represents the FC open circuit voltage, while the three last terms represent reductions in this voltage to supply the useful voltage of the cell V_{FC}, for a certain operating condition. Each one of the terms can be calculated by the following equations,

$$\begin{aligned} V_{act} &= A\log\left(\frac{i_{FC}-i_n}{i_0}\right) \\ V_{ohm} &= R_m\left(i_{FC}-i_n\right) \\ V_{concent} &= b\log\left(1-\frac{i_{FC}-i_n}{i_{lim}}\right) \end{aligned} \quad (5)$$

Hence, i_{FC} is the delivered current, i_0 is the exchange current, A is the slope of the Tafel line, i_{Lim} is the limiting current, B is the constant in the mass transfer, i_n is the internal current and R_m is the membrane and contact resistances.

2.2. Electric Double-layer supercapacitors

A. Principle

The basic principle of electric double-layer capacitors lies in capacitive properties of the interface between a solid electronic conductor and a liquid ionic conductor. These properties discovered by Helmholtz in 1853 lead to the possibility to store energy at solid/liquid interface. This effect is called electric double-layer, and its thickness is limited to some nanometers (Belhachemi et al., 2000).

Energy storage is of electrostatic origin, and not of electrochemical origin as in the case of accumulators. So, supercapacitors are therefore capacities, for most of marketed devices. This gives them a potentially high specific power, which is typically only one order of magnitude lower than that of classical electrolytic capacitors.

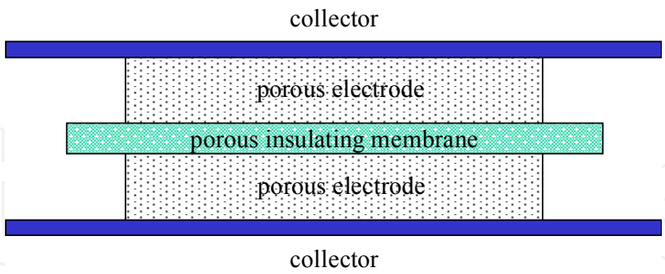

Fig. 5. Principle of assembly of the supercapacitors

In SCs, the dielectric function is performed by the electric double-layer, which is constituted of solvent molecules. They are different from the classical electrolytic capacitors mainly because they have a high surface capacitance (10-30 μF.cm^{-2}) and a low rated voltage limited by solvent decomposition (2.5 V for organic solvent). Therefore, to take advantage of electric double-layer potentialities, it is necessary to increase the contact surface area between electrode and electrolyte, without increasing the total volume of the whole.

The most widespread technology is based on activated carbons to obtain porous electrodes with high specific surface areas (1000-3000 $m^2.g^{-1}$). This allows obtaining several hundred of farads by using an elementary cell.

SCs are then constituted, as schematically presented below in Fig. 5, of:

- two porous carbon electrodes impregnated with electrolyte,
- a porous insulating membrane, ensuring electronic insulation and ionic conduction between electrodes,
- metallic collectors, usually in aluminium.

B. Modeling and sizing of suparcpacitors

Many applications require that capacitors be connected together, in series and/or parallel combinations, to form a "bank" with a specific voltage and capacitance rating. The most critical parameter for all capacitors is voltage rating. So they must be protected from over voltage conditions. The realities of manufacturing result in minor variations from cell to cell. Variations in capacitance and leakage current, both on initial manufacture and over the life of the product, affect the voltage distribution. Capacitance variations affect the voltage distribution during cycling, and voltage distribution during sustained operation at a fixed voltage is influenced by leakage current variations. For this reason, an active voltage balancing circuit is employed to regulate the cell voltage.

It is common to choose a specific voltage and thus calculating the required capacitance. In analyzing any application, one first needs to determine the following system variables affecting the choice of SC,

-the maximum voltage, V_{SCMAX}
-the working (nominal) voltage, V_{SCNOM}
-the minimum allowable voltage, V_{SCMIN}
-the current requirement, I_{SC}, or the power requirement, P_{SC}
-the time of discharge, t_d
-the time constant
-the capacitance per cell, C_{SCcell}
-the cell voltage, V_{SCcell}
-the number of cell needs, n

To predict the behavior of SC voltage and current during transient state, physics-based dynamic models (a very complex charge/discharge characteristic having multiple time constants) are needed to account for the time constant due to the double-layer effects in SC. The reduced order model for a SC cell is represented in Fig. 6. It is comprised of four ideal circuit elements: a capacitor C_{SCcell}, a series resistor R_S called the equivalent series resistance (ESR), a parallel resistor R_P and a series stray inductor L of ~nH. The parallel resistor R_P models the leakage current found in all capacitors.

This leakage current varies starting from a few milliamps in a big SC under a constant current as shown in Fig. 7.

A constant discharging current is particularly useful when determining the parameters of the SC.

Nevertheless, Fig. 7 should not be used to consider sizing SCs for constant power applications, such as common power profile used in hybrid source.

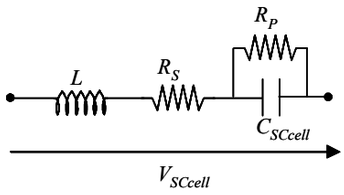

Fig. 6. Simple model of a supercapacitor cell

To estimate the minimum capacitance C_{SCMIN}, one can write an energy equation without losses (R_{ESR} neglected) as,

$$\frac{1}{2}C_{SCMIN}\left(V_{SCNOM}^2 - V_{SCMIN}^2\right) = P_{SC}t \tag{6}$$

with

$$P_{SC}(t) = V_{SC}(t)i_{SC}(t) \tag{7}$$

Then,

$$C_{SCMIN} = \frac{2P_{SC}t_d}{V_{SCNOM}^2 - V_{SCMIN}^2} \tag{8}$$

From (6) and (7), the instantaneous capacitor voltage and current are described as,

$$\begin{cases} V_{SC}(t) = V_{SCNOM}\sqrt{1-\left(1-\left(\dfrac{V_{SCNOM}}{V_{SCMIN}}\right)^2\right)\dfrac{t}{t_d}} \\ i_{SC}(t) = \dfrac{P_{SC}}{\sqrt{1-\left(1-\left(\dfrac{V_{SCNOM}}{V_{SCMIN}}\right)^2\right)\dfrac{t}{t_d}}} \end{cases} \tag{9}$$

Since the power being delivered is constant, the minimum voltage and maximum current can be determined based on the current conducting capabilities of the SC. (6) and (7) can then be rewritten as,

$$\begin{cases} V_{SCMIN} = \sqrt{V_{SCNOM}^2 - \dfrac{2P_{SC}t_d}{C_{MIN}}} \\ I_{SCMIN} = \dfrac{P_{SC}}{\sqrt{V_{SCNOM}^2 - \dfrac{2P_{SC}t_d}{C_{MIN}}}} \end{cases} \tag{10}$$

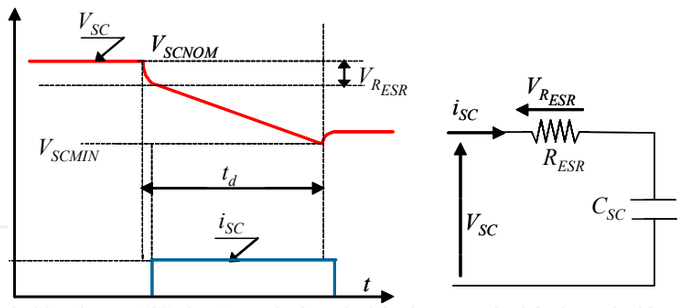

Fig. 7. Discharge profile for a SC under constant current.

The variables V_{SCMAX} and C_{SC} are indeed related by the number of cells n. The assumption is that the capacitors will never be charged above the combined maximum voltage rating of all the cells. Thus, we can introduce this relationship with the following equations,

$$\begin{cases} V_{SCMAX} = nV_{SCcell} \\ C_{SC} = \dfrac{C_{SCcell}}{n} \end{cases} \tag{11}$$

Generally, V_{SCMIN} is chosen as V_{SCMAX} /2, from (6), resulting in 75% of the energy being utilized from the full-of-charge (*SOC*[1] = 100%). In applications where high currents are drawn, the effect of the R_{ESR} has to be taken into account. The energy dissipated W_{loss} in the R_{ESR}, as well as in the cabling, and connectors could result in an under-sizing of the number of capacitors required. For this reason, knowing SC current from (6), one can theoretically calculate these losses as,

$$W_{loss} = \int_0^{t_d} i_C^2(\tau) R_{ESR} d\tau = P_{SC} R_{ESR} C_{MIN} \ln\left(\frac{V_{SCNOM}}{V_{SCMIN}}\right) \tag{12}$$

To calculate the required capacitance C_{SC}, one can rewrite (6) as,

$$\frac{1}{2} C_{SCMIN}\left(V_{SCMAX}^2 - V_{SCMIN}^2\right) = P_{SC} t + W_{loss} \tag{13}$$

From (6) and (13), one obtains

$$\begin{cases} C_{SC} = C_{SCMIN}(1 + X) \\ X = \dfrac{W_{loss}}{P_{SC} t} \end{cases} \tag{14}$$

where X is the energy ratio.
From the equations above, an iterative method is needed in order to get the desired optimum value.

[1] State Of Charge

C. State of the art and potential application

Developed at the end of the seventies for signal applications (for memory back-up for example), SCs had at that time a capacitance of some farads and a specific energy of about 0.5 $Wh.kg^{-1}$.

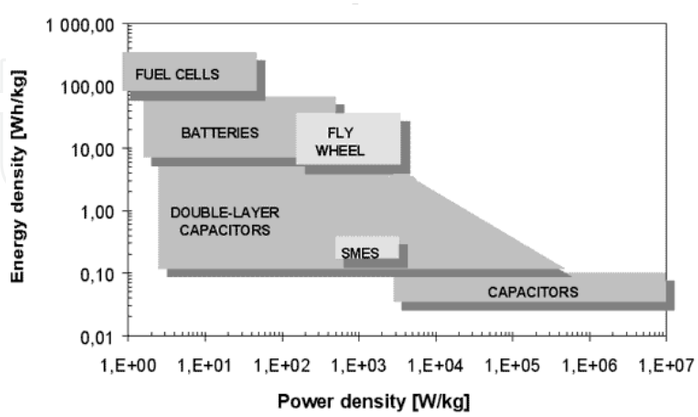

Fig. 8. Comparison between capacitors, supercapacitors, batteries and Fuel cell

High power SCs appear during the nineties and bring high power applications components with capacitance of thousand of farads and specific energy and power of several $Wh.kg^{-1}$ and $kW.kg^{-1}$.

In the energy-power plan, electric double layers SCs are situated between accumulators and traditional capacitors.

Then these components can carry out two main functions:

- the function "source of energy", where SCs replace electrochemical accumulators, the main interest being an increase in reliability,
- the function "source of power", for which SCs come in complement with accumulators (or any other source limited in power), for a decrease in volume and weight of the whole system.

2.3. State of the art of battery in electric vehicles

An electric vehicle (EV) is a vehicle that runs on electricity, unlike the conventional vehicles on road today which are major consumers of fossil fuels like gasoline. This electricity can be either produced outside the vehicle and stored in a battery or produced on board with the help of FC's.

The development of EV's started as early as 1830's when the first electric carriage was invented by Robert Andersen of Scotland, which appears to be appalling, as it even precedes the invention of the internal combustion engine (ICE) based on gasoline or diesel which is prevalent today. The development of EV's was discontinued as they were not very convenient and efficient to use as they were very heavy and took a long time to recharge.

This led to the development of gasoline based vehicles as the one pound of gasoline gave equal energy as a hundred pounds of batteries and it was relatively much easier to refuel and use gazoline. However, we today face a rapid depletion of fossil fuel and a major concern over the noxious green house gases their combustion releases into the atmosphere causing long term global crisis like climatic changes and global warming. These concerns

are shifting the focus back to development of automotive vehicles which use alternative fuels for operations. The development of such vehicles has become imperative not only for the scientists but also for the governments around the globe as can be substantiated by the Kyoto Protocol which has a total of 183 countries ratifying it (As on January 2009).

A. Batteries technologies

A battery is a device which converts chemical energy directly into electricity. It is an electrochemical galvanic cell or a combination of such cells which is capable of storing chemical energy. The first battery was invented by Alessandro Volta in the form of a voltaic pile in the 1800's. Batteries can be classified as primary batteries, which once used, cannot be recharged again, and secondary batteries, which can be subjected to repeated use as they are capable of recharging by providing external electric current. Secondary batteries are more desirable for the use in vehicles, and in particular traction batteries are most commonly used by EV manufacturers. Traction batteries include Lead Acid type, Nickel and Cadmium, Lithium ion/polymer , Sodium and Nickel Chloride, Nickel and Zinc.

	Lead Acid	Ni - Cd	Ni - MH	Li – Ion	Li - polymer	Na - $NiCl_2$	Objectives
Specific Energy (Wh/Kg)	35 – 40	55	70 – 90	125	155	80	200
Specific Power (W/Kg)	80	120	200	260	315	145	400
Energy Density (Wh/m^3)	25 – 35	90	90	200	165	130	300
Cycle Life (No. of charging cycles)	300	1000	600	+ 600	+ 600	600	1000

Table 1. Comparison between different baterries technologies.

The battery for electrical vehicles should ideally provide a high autonomy (i.e. the distance covered by the vehicle for one complete discharge of the battery starting from its potential) to the vehicle and have a high specific energy, specific power and energy density (i.e. light weight, compact and capable of storing and supplying high amounts of energy and power respectively). These batteries should also have a long life cycle (i.e. they should be able to discharge to as near as it can be to being empty and recharge to full potential as many number of times as possible) without showing any significant deterioration in the performance and should recharge in minimum possible time. They should be able to operate over a considerable range of temperature and should be safe to handle, recyclable with low costs. Some of the commonly used batteries and their properties are summarized in the Table 1.

B. Principle

A battery consists of one or more voltaic cell, each voltaic cell consists of two half-cells which are connected in series by a conductive electrolyte containing anions (negatively charged ions) and cations (positively charged ions). Each half-cell includes the electrolyte and an electrode (anode or cathode). The electrode to which the anions migrate is called the anode and the electrode to which cations migrate is called the cathode. The electrolyte connecting these electrodes can be either a liquid or a solid allowing the mobility of ions.

In the redox reaction that powers the battery, reduction (addition of electrons) occurs to cations at the cathode, while oxidation (removal of electrons) occurs to anions at the anode. Many cells use two half-cells with different electrolytes. In that case each half-cell is enclosed in a container, and a separator that is porous to ions but not the bulk of the electrolytes prevents mixing. The figure 10 shows the structure of the structure of Lithium–Ion battery using a separator to differentiate between compartments of the same cell utilizing two respectively different electrolytes

Each half cell has an electromotive force (or emf), determined by its ability to drive electric current from the interior to the exterior of the cell. The net emf of the battery is the difference between the emfs of its half-cells. Thus, if the electrodes have emfs E_1 and E_2, then the net emf is $E_{cell} = E_2 - E_1$. Therefore, the net emf is the difference between the reduction potentials of the half-cell reactions.

The electrical driving force or ΔV_{Bat} across the terminals of a battery is known as the terminal voltage and is measured in volts. The terminal voltage of a battery that is neither charging nor discharging is called the open circuit voltage and equals the emf of the battery.

An ideal battery has negligible internal resistance, so it would maintain a constant terminal voltage until exhausted, then dropping to zero. If such a battery maintained 1.5 volts and stored a charge of one Coulomb then on complete discharge it would perform 1.5 Joule of work.

$$\text{Work done by battery (W)} = \text{- Charge X Potential Difference} \tag{15}$$

$$\text{Charge} = \frac{\text{Coulomb}}{\text{Mole} \quad \text{Electrons}} \text{Moles} \quad \text{Electrons} \tag{16}$$

$$W = -nFEcell \tag{17}$$

Where n is the number of moles of electrons taking part in redox, $F = 96485$ coulomb/mole is the Faraday's constant i.e. the charge carried by one mole of electrons.

The open circuit voltage, E_{cell} can be assumed to be equal to the maximum voltage that can be maintained across the battery terminals. This leads us to equating this work done to the Gibb's free energy of the system (which is the maximum work that can be done by the system)

$$\Delta G = W\max = -nFEcell \tag{18}$$

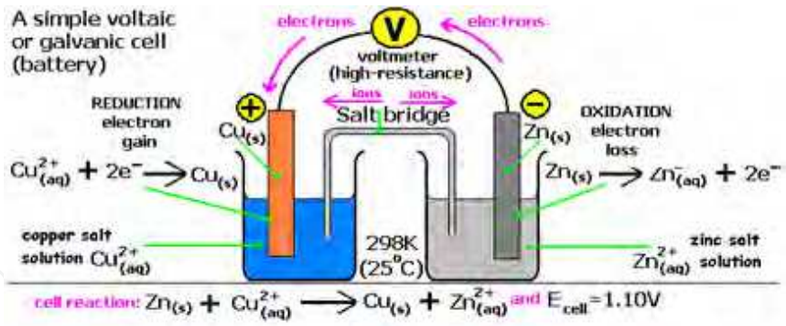

Fig. 9. Showing the apparatus and reactions for a simple galvanic Electrochemical Cell

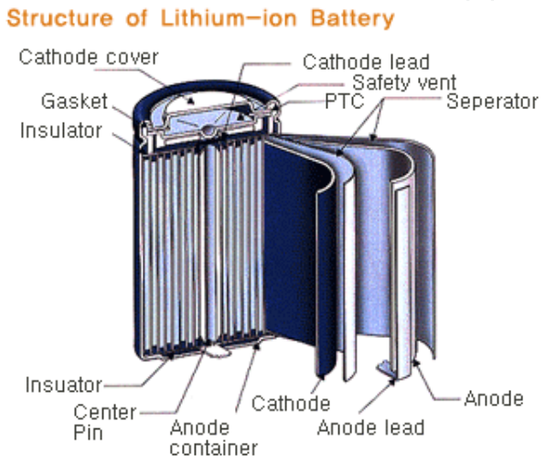

Fig. 10. Structure of Lithium-Ion Battery

C. Model of Battery

Non Idealities in Batteries: Electrochemical batteries are of great importance in many electrical systems because the chemical energy stored inside them can be converted into electrical energy and delivered to electrical systems, whenever and wherever energy is needed. A battery cell is characterized by the open-circuit potential (V_{OC}), i.e. the initial potential of a fully charged cell under no-load conditions, and the cut-off potential (V_{cut}) at which the cell is considered discharged. The electrical current obtained from a cell results from electrochemical reactions occurring at the electrode-electrolyte interface. There are two important effects which make battery performance more sensitive to the discharge profile:

- Rate Capacity Effect: At zero current, the concentration of active species in the cell is uniform at the electrode-electrolyte interface. As the current density increases the concentration deviates from the concentration exhibited at zero current and state of charge as well as voltage decrease (Rao et al., 2005)
- Recovery Effect: If the cell is allowed to relax intermittently while discharging, the voltage gets replenished due to the diffusion of active species thereby giving it more life (Rao et al., 2005)

D. Equivalent Electrical Circuit of Battery

Many electrical equivalent circuits of battery are found in literature. (Chen at al., 2006) presents an overview of some much utilized circuits to model the steady and transient behavior of a battery. The Thevenin's circuit is one of the most basic circuits used to study the transient behavior of battery is shown in figure 11.

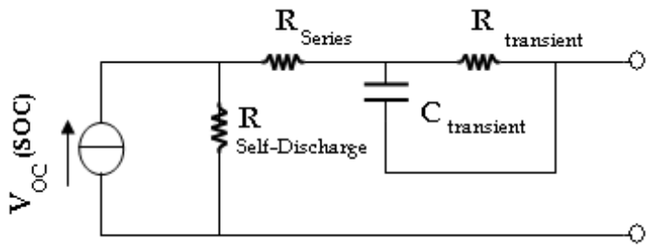

Fig. 11. Thevenin's model

It uses a series resistor (R_{series}) and an RC parallel network ($R_{transient}$ and $C_{transient}$) to predict the response of the battery to transient load events at a particular state of charge by assuming a constant open circuit voltage [V_{oc}(SOC)] is maintained. This assumption unfortunately does not help us analyze the steady-state as well as runtime variations in the battery voltage. The improvements in this model are done by adding more components in this circuit to predict the steady-state and runtime response. For example, (Salameh at al., 1992) uses a variable capacitor instead of V_{oc} (SOC) to represent nonlinear open circuit voltage and SOC, which complicates the capacitor parameter.

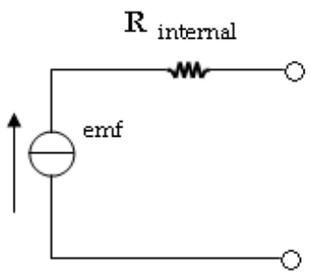

Fig. 12. Circuit showing battery emf and internal resistance $R_{internal}$

However, in our study we are mainly concerned with the recharging of this battery which occurs while breaking. The SC coupled with the battery accumulates high amount of charge when breaks are applied and this charge is then utilized to recharge the battery. Therefore, the design of the battery is kept to a simple linear model which takes into account the internal resistance ($\mathbf{R}_{internal}$) of the battery and assumes the emf to be constant throughout the process (Figure. 12).

3. Control of the Electric Vehicles based on FC, SCs and Batteries on the DC Link

3.1 Structure of the hybrid source

As shown in Fig. 13 the studied system comprises a DC link directly supplied by batteries, a PEMFC connected to the DC link by means of a Boost converter, and a supercapacitive storage device connected to the DC link through a current reversible DC-DC converter. The function of FC and the batteries is to supply mean power to the load, whereas the storage device is used as a power source: it manages load power peaks during acceleration and braking.

The aim is to have a constant DC voltage and the challenge is to maintain a constant power working mode for the main sources (batteries and FC).

3.2. Problem formulation

The main objectives of the proposed study are:

- To compare two control techniques of the hybrid source by controlling the two DC-DC converters. The first is based on passivity control by using voltage control (on FC and current control for SC), and the second is based on sliding mode control by using current controller.
- To maintain a constant mean energy delivered by the FC, without a significant power peak, and to ensure the transient power is supplied by the SCs.
- To recover energy through the charge of the SC.

After system modelling, equilibrium points are computed in order to ensure the desired behaviour of the system. When steady state is reached, the load has to be supplied only by the FC source. So the controller has to maintain the DC bus voltage to a constant value and the SCs current has to be cancelled. During transient, the power delivered by the DC source has to be the more constant as possible (without a significant power peak), so the SCs deliver the transient power to the load. If the load provides current, the SCs recover its energy.

At equilibrium, the SC has to be charged and the current has to be equal to zero.

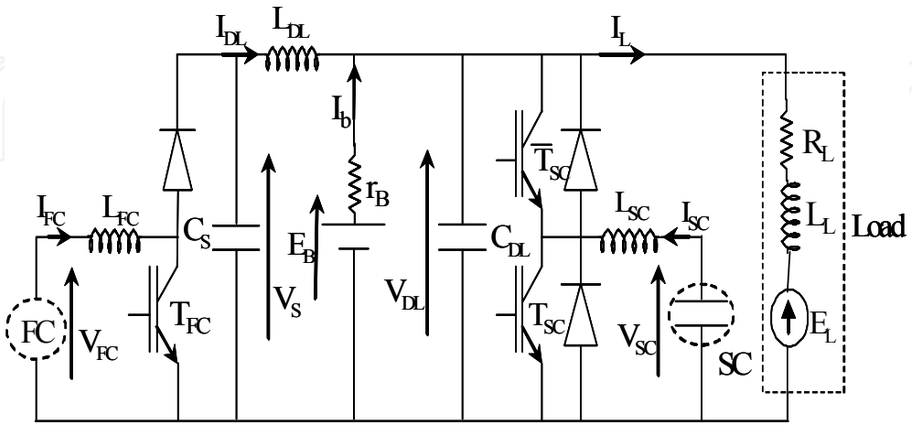

Fig. 13. Structure of the hybrid source

3.3 Port Controlled Hamiltonian System

PCH systems were introduced by van der Schaft and Maschke in the early nineties, and have since grown to become a large field of interest in the research of electrical, mechanical and electro-mechanical systems. A recent and very interesting approach in PBC is the Interconnection and Damping Assignment (IDA-PBC) method, which is a general way of stabilizing a large class of physical systems) (Ortega et al. 2002) (Becherif et al., 2005).

A. Equations of the system

The overall model of the hybrid system is written in a state space equation by choosing the following state space vector:

$$\begin{aligned} x &= \begin{bmatrix} x_1 & x_2 & x_3 & x_4 & x_5 & x_6 & x_7 \end{bmatrix}^T \\ &= \begin{bmatrix} V_S & I_{FC} & V_{DL} & I_{DL} & V_{SC} & I_{SC} & I_L \end{bmatrix}^T \end{aligned} \tag{19}$$

The output voltage of a single cell V_{FC} can be defined as the result of the following expression:

$$V_{FC} = E_0 - A\log\left(\frac{i_{FC} - i_n}{i_0}\right) - \left\{R_m(i_{FC} - i_n) + B\log\left(1 - \frac{i_{FC} - i_n}{i_{Lim}}\right)\right\} \tag{20}$$

where E is the thermodynamic potential of the cell representing its reversible voltage, i_{FC} is the delivered current, i_o is the exchange current, A is the slope of the Tafel line, i_{Lim} is the limiting current, B is the constant in the mass transfer, i_n is the internal current and R_m is the membrane and contact resistances. Hence $V_{FC} = f(i_{FC})$.

The fourth term represents the voltage drop resulting from the concentration or mass transportation of the reacting gases.

In equation (20), the first term represents the FC open circuit voltage, while the three last terms represent reductions in this voltage to supply the useful voltage of the cell V_{FC}, for a certain operating condition. Each of the terms can be calculated by the following equations,

The control vector is:

$$\begin{aligned} \mu &= \begin{bmatrix} \mu_1, & \mu_2 \end{bmatrix}^T = \begin{bmatrix} (1 - U_{FC}), & (1 - U_{SC}) \end{bmatrix}^T \\ \text{or } U &= \begin{bmatrix} U_{FC}, & U_{SC} \end{bmatrix}^T \end{aligned} \tag{21}$$

With $V_{FC}=V_{FC}(x_2)$ given in (Larminie & Dicks, 2000). In the sequel, V_{FC} will be considered as a measured disturbance, and from physical consideration, it comes that $V_{FC} \in [0; V_d[$.

B. Equilibrium

After simple calculations the equilibrium vector is:

$$\begin{aligned}\bar{x} &= \left[\bar{x}_1,\ \bar{x}_2,\ \bar{x}_3,\ \bar{x}_4,\ \bar{x}_5,\ \bar{x}_6,\ \bar{x}_7\right]^T \\ &= \left[V_d,\ \left(\frac{V_d}{V_{FC}}\left(\frac{V_d}{R_L}-\frac{E_B-V_d}{r_B}\right)\right),\ V_d,\ \frac{V_d}{R_L}-\frac{E_B-V_d}{r_B},\ V_{SC}(t=0),\ 0,\ \frac{V_d}{R_L}\right]^T\end{aligned} \tag{22}$$

where V_d is the desired DC link voltage. An implicit purpose of the proposed structure shown in Fig.13 is to recover energy to charge the SC. Hence, the desired voltage $\bar{x}_5 = \bar{V}_{SC} = V_{SC}(t=0)$=Constante.

$$\bar{\mu} = \left[\bar{\mu}_1,\ \bar{\mu}_2\right]^T = \left[\frac{V_{FC}}{V_d},\ \frac{\bar{x}_5}{V_d}\right]^T \tag{23}$$

Or

$$\bar{U} = \left[\bar{U}_{FC},\ \bar{U}_{SC}\right]^T = \left[1-\frac{V_{FC}}{V_d},\ 1-\frac{\bar{x}_5}{V_d}\right]^T \tag{24}$$

The natural energy function of the system is:

$$H = \frac{1}{2}x^T Q x \tag{25}$$

where

$$Q = \mathrm{diag}\left\{C_S;\ L_{Fc};\ C_{DL};\ L_{DL};\ C_{SC};\ L_{SC};\ L_L\right\}$$

is a diagonal matrix.

C. Port-Controlled Hamiltonian representation of the system

In the following, a closed loop PCH representation is given. The desired closed loop energy function is:

$$H_d = \frac{1}{2}\tilde{x}^T Q \tilde{x} \tag{26}$$

Where $\tilde{x} = x - \bar{x}$ is the new state space defining the error between the state x and its equilibrium value $\bar{x}$.

The PCH form of the studied system with the new variable $\tilde{x}$ as a function of the gradient of the desired energy (26) is:

$$\dot{\tilde{x}} = \left[\Im(\mu_1,\mu_2) - \Re\right]\nabla H_d + A_i(\bar{x},\mu) \tag{27}$$

With

$$\Im(\mu_1,\mu_2)-\Re=$$

$$\begin{bmatrix} 0 & \frac{\mu_1}{C_S L_{FC}} & 0 & \frac{1}{C_S L_{DL}} & 0 & 0 & 0 \\ \frac{-\mu_1}{C_S L_{FC}} & 0 & 0 & 0 & 0 & 0 & 0 \\ 0 & 0 & \frac{-1}{C_{DL}^2 r_B} & \frac{1}{C_{DL} L_{DL}} & 0 & \frac{\mu_2}{C_{DL} L_{SC}} & \frac{-1}{C_{DL} L_L} \\ \frac{1}{C_S L_{DL}} & 0 & \frac{-1}{C_{DL} L_{DL}} & 0 & 0 & 0 & 0 \\ 0 & 0 & 0 & 0 & 0 & \frac{-1}{C_{SC} L_{SC}} & 0 \\ 0 & 0 & \frac{-\mu_2}{C_{DL} L_{SC}} & 0 & \frac{1}{C_{SC} L_{SC}} & 0 & 0 \\ 0 & 0 & \frac{1}{C_{DL} L_L} & 0 & 0 & 0 & \frac{-R_L}{L_L^2} \end{bmatrix} \tag{28}$$

And

$$\nabla H_d = \begin{bmatrix} C_S \tilde{x}_1 \\ L_{FC} \tilde{x}_2 \\ C_{DL} \tilde{x}_3 \\ L_{DL} \tilde{x}_4 \\ C_{SC} \tilde{x}_5 \\ L_{SC} \tilde{x}_6 \\ L_L \tilde{x}_7 \end{bmatrix} \tag{29}$$

$$A_i(\bar{x},\mu) = \begin{bmatrix} C_S\left[-\bar{x}_4 + \mu_1 \bar{x}_2\right] \\ \frac{1}{L_{FC}}\left[V_{FC} - \mu_1 \bar{x}_1\right] \\ 0 \\ 0 \\ 0 \\ \frac{1}{L_{SC}}\left[\bar{x}_5 - \mu_2 \bar{x}_3\right] \\ 0 \end{bmatrix} \tag{30}$$

Where

$$\Im(\mu_1,\mu_2) = -\Im^T(\mu_1,\mu_2) \tag{31}$$

is a skew symmetric matrix defining the interconnection between the state space and $\Re = \Re^T \geq 0$ is a symmetric positive semi definite matrix defining the damping of the system.

With *r* is a design parameter, the following control laws are proposed:

$$\mu_1 = \bar{\mu}_1 \quad \text{and} \quad \mu_2 = \bar{\mu}_2 + r\tilde{x}_6 \tag{32}$$

Proposition 1: The origin of the closed loop PCH system (27), with the control laws (32) and (23) with the radially unbounded energy function (26), is globally stable.
Proof: The closed loop dynamic of the PCH system (27) with the laws (32) and (23) with the radially unbounded energy function (26) is:

$$\dot{\tilde{x}} = \left[\Im(\mu_1, \mu_2) - \Re'\right]\nabla H_d \tag{33}$$

where

$$\Re' = diag\left\{0; \quad 0; \quad \frac{1}{\left(C_{DL}^2 r_B\right)}; \quad 0; \quad 0; \quad \frac{rV_d}{L_{SC}^2}; \frac{R_L}{L_L^2} \right\} = \Re'^T \geq 0 \tag{34}$$

The derivative of the desired energy function (26) along the trajectory of (33) is:

$$\dot{H}_d = \nabla H_d^T \dot{\tilde{x}} = -\nabla H_d^T \Re' \nabla H_d \leq 0 \tag{35}$$

3.4 Sliding mode control of the system

Due to the weak request on the FC, a classical PI controller is adapted for the boost converter. Because of the fast response in the transient power and the possibility to work with a variable or a constant frequency, a non-linear sliding mode control (ayad et al, 2007) which allows management of the charge and discharge of the SC tank is chosen for the DC-DC bidirectional SC converter.
The current supplied by the FC is limited to an interval [I_{MIN}, I_{MAX}]. Within this interval, the FC boost ensures the regulation of this current to its reference. But, as soon as the load current is greater than I_{MAX} or lower than I_{MIN}, the boost becomes unable to regulate the desired current. The lacking or excess current is then provided or absorbed by the storage device, hence the DC link current is kept equal to its reference level. Consequently, three modes can be defined to optimize the function of the hybrid source:
- The normal mode, for which the load current is within the interval [I_{MIN}, I_{MAX}]. In this mode, the boost ensures the regulation of the DC link current, and the control of the bidirectional SC converter leads to the charge or the discharge of SC up to a reference voltage level V_{SCREF},
- The discharge mode, for which the load current is greater than I_{MAX}. The current reference of the boost is then saturated to I_{MAX}, and the DC-DC converter ensures the regulation of the DC link current by supplying the lacking current through the SC discharge,
- The recovery mode, for which the load current is lower than I_{MIN}. The power reference of the controlled rectifier is then saturated to I_{MIN} and the DC-DC converter ensures the regulation of the DC link current by absorbing the excess current through the SC charge.

A. DC-DC Fuel Cell converter control principle

The FC current reference I_{FC}^* is generated by means of a PI current loop control on a DC link current and load current. The switching device is controlled by a hysterisis comparator.

$$I_{FC}^* = k_p\left(I_L - I_{DL}\right) + k_I \int_0^t \left(I_L - I_{DL}\right) dt \tag{36}$$

where k_p and k_i are the proportional and integral gains.

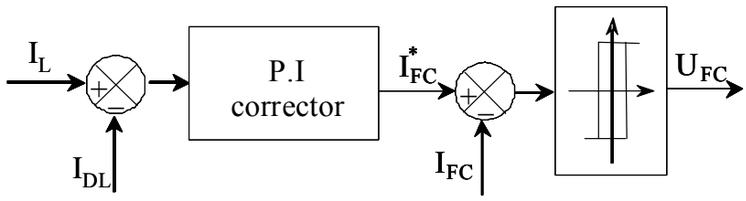

Fig. 14. Control of the FC converter

B. DC-DC Supercapacitors converter control principle

To ensure proper function for the three modes, we use a sliding mode control for the bidirectional SC converter. Thus we define a sliding surface S as a function of the DC link current I_{DL}, the load current I_L, the SC voltage V_{SC}, its reference V_{SC}^* and the SC current I_{SC}:

$$S = \left(I_{DL} - I_L\right) + k_C\left(I_{SC} - I\right) \tag{37}$$

with

$$I = k_{ps}\left(V_{SC} - V_{SC}^*\right) + k_{is}\int_0^t \left(V_{SC} - V_{SC}^*\right)dt \tag{38}$$

With, k_{ps} and k_{is} are the proportional and integral gains.

When $S < 0$, the lower $T_{SC}=1$ in Fig.14 is switched on, and the upper $\overline{T}_{SC} = 0$ is switched off. When $S > 0$, the upper $\overline{T}_{SC} = 1$ is switched on and the lower $T_{SC}=0$ is switched off.

The FC PI controller ensures that I_{DL} tracks I_L. The SC PI controller ensures that V_{SC} tracks its reference V_{SC}^*.

k_C is the coefficient of proportionality, which ensures that the sliding surface equals zero by tracking the SC currents to its reference I when the FC controller cannot ensure I_{DL} tracks I_L.

In steady state conditions, the FC converter ensures that the first term of the sliding surface is zero, and the integral term of equation (38) implies that $V_{SC} = V_{SC}^*$. Then, imposing $S = 0$ leads to $I_{SC} = 0$, as far as the boost converter output current I_{DL} is not limited so that the storage element supplies energy only during power transient and I_{DL} limitation.

The general system of the DC link and the DC-DC SC converter equations can be written as:

$$\dot{X} = AX + BU + C + \xi \tag{39}$$

With

$$X = \left[V_{DL} \quad I_{SC} \quad V_{SC} \quad I\right]^T$$

And

$$A = \begin{bmatrix} -1/(r_B.C_{DL}) & 1/C_{DL} & 0 & 0 \\ -1/L_{SC} & -r_{SC}/L_{SC} & 1/L_{SC} & 0 \\ 0 & -1/C_{SC} & 0 & 0 \\ 0 & -k_{ps}/C_{SC} & k_{is} & 0 \end{bmatrix}$$

$$B = \begin{bmatrix} \frac{-I_{SC}}{C_{DL}} & \frac{V_{DL}}{L_{SC}} & 0 & 0 \end{bmatrix}^T$$

$$,\xi = \begin{bmatrix} \frac{(I_{DL} - I_L)}{C_{DL}} & 0 & 0 & 0 \end{bmatrix}^T \quad C = \begin{bmatrix} \frac{E_B}{(r_B C_{DL})} & 0 & 0 & -k_{is} V_{SC}^* \end{bmatrix}^T,$$

$$U = U_{SC}$$

If we denote

$$G = \begin{bmatrix} 0 & k_C & 0 & -k_C \end{bmatrix} \tag{40}$$

the sliding surface is then given by

$$S = C_{DL}\xi + GX \tag{41}$$

In order to set the system dynamics, we define the reaching law

$$\dot{S} = -\lambda S - K\,\mathrm{sign}(S) \tag{42}$$

with

$$K = 0 \quad \text{if } \|S\| < \varepsilon \text{ and } K = n\lambda\varepsilon \quad \text{if } \|S\| > \varepsilon \tag{43}$$

The linear term $-\lambda S(X)$ imposes the dynamics inside the error bandwidthε. The choice of a high value of λ ($\leq f_C/2$) ensures a small static error when $\|S\| < \varepsilon$. The non-linear term $-K\mathrm{sign}(S)$ permits to reject perturbation effects (uncertainty of the model, variations of the working conditions…). This term allows compensation high values of error $\|S\| > \varepsilon$ due to the above mentioned perturbations. The choice of a small value of ε leads to high current ripple (chattering effect) but the static error remains small. A high value of ε forces a reduction in the value of λ to ensure the stability of the system and leads to a higher static error.

Once the parameters (λ, K, ε) of the reaching law are determined, it is possible to calculate the continuous equivalent control, which allows the state trajectory on the sliding surface to be maintained. Using Equations (39), (41) and (42), we find:

$$U_{SCeq} = (GB)^{-1}\left\{-GAX - GC - \lambda GX - K\,\mathrm{sign}(S) - C_{DL}\left[\dot{\xi} + \lambda\xi\right]\right\} \tag{44}$$

(37) and (39) give the equation:

$$A_{eq} = A - B(GB)^{-1}GA - B(GB)^{-1}\lambda G \tag{45}$$

This equation allows the determination of the poles of the system during the sliding motion as a function of λ and k_C. The parameters k_{is} and k_{ps} are then determined by solving S = 0.

This equation is justified by the fact that the sliding surface dynamic is much greater than the SC voltage variation.

C. Stability

Consider the following Lyapunov function:

$$V = \frac{1}{2}S^2 \tag{46}$$

Where, S is the sliding surface.
The derivative of the Lyapunov function along the trajectory of (42) in the closed loop with the control (44) gives:

$$\dot{V} = S\dot{S} = -\lambda S^2 - KSsign(S) \leq 0 \tag{47}$$

With $\lambda, K > 0$
Hence, the origin of the closed loop of the system (39) with the control (44) and the sliding surface (41) is asymptotically stable.

3.5 Simulation results of the hybrid source control

The whole system has been implemented in MATLAB-SIMULINK with the following parameters associated to the hybrid sources:
- FC parameters: P_{MAX} = 400 W.
- DC link parameters: V_{DL}= 24 V.
- SC parameters: C_{SC} = 3500/6 F, $V_{SC}^{*} = 15V$.

The results presented in this section have been carried out by connecting the hybrid source to a "R, L and E_L " load.

A. Sliding mode control applied to the hybrid source

Figures 15, 16 and 17 present the behaviour of currents I_{DL}, I_{DL}, I_{SC}, I_B and the DC link voltage V_{DL} for transient responses obtained for a transition from the normal mode to the discharge mode by using sliding mode control. The test is performed by changing sharply the e.m.f load voltage E_L in the interval of $t \in [0.5\ s, 1.5\ s]$. The load current I_L changes from 16.8 A to 25 A. The current load I_L = 16.8 A corresponds to a normal mode and the current load I_L = 25 A to a discharge mode.
At the starting of the system, only the FC provides the mean power to the load. The storage device current reference is equal to zero, we are in normal mode. In the transient state, the load current I_L became greater then the DC link current I_{DL}. The storage device current reference became positive thanks to control function which compensate this positive value by the difference between the SC voltage and its reference. We are in discharging mode. After the load variation (t > 1.5 s), the current in the DC link became equal to the load current. The SC current I_{SC} became null. We have a small variation in the batteries currents.

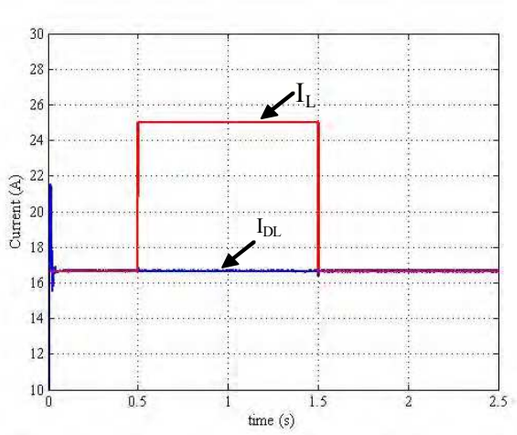

Fig. 15. Load and DC link currents

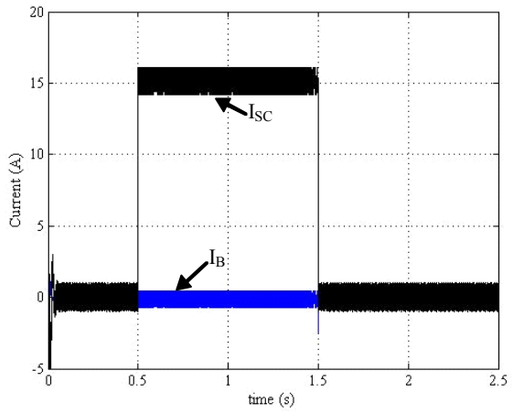

Fig. 16. SC and batteries currents

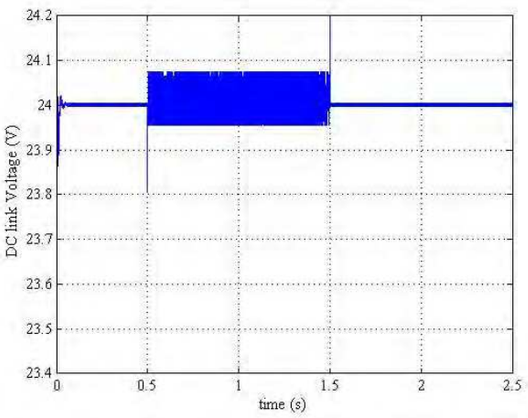

Fig. 17. DC link voltage

B. Passivity Based Control applied to the hybrid source

Figure 18 shows the FC voltage and current. Figure 19 presents the SC voltage and current response. The SC supply power to the load in the transient and in the steady state no power or energy is extracted since the current $x_6 = I_{SC}$ is null.

The positive sens of I_{SC} means that the SCs supply the load and the negative one corresponds to the recover of energy from the FC to the SC. Figure 20 presents the batteries voltage and its current. Figure 21 presents the response of the system to changes in the load current I_L. The DC Bus voltage tracks well the reference, i.e. very low overshoot and no steady state error are observed. It can be seen from this figure that the system with the proposed controller is robust towards load resistance changes. Figure 22 shows the FC Boost controller, the SC bidirectional converter controller and the changes in the Load resistance RL. U_{SC} and U_{FC} are in the set [0; 1].

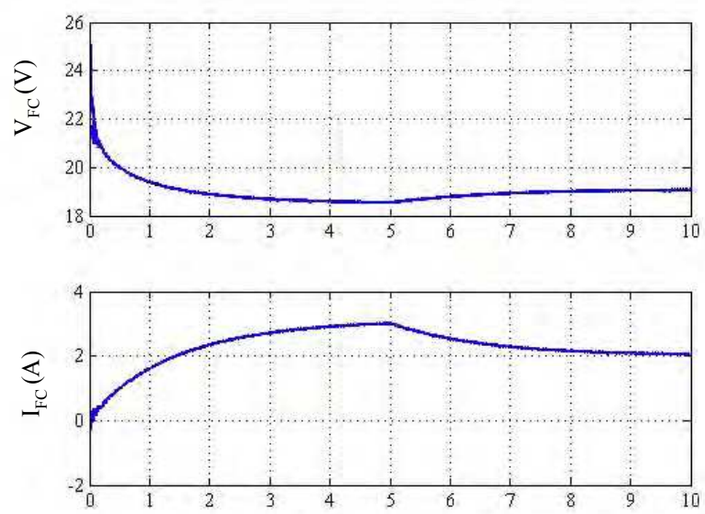

Fig. 18. FC voltage and FC current

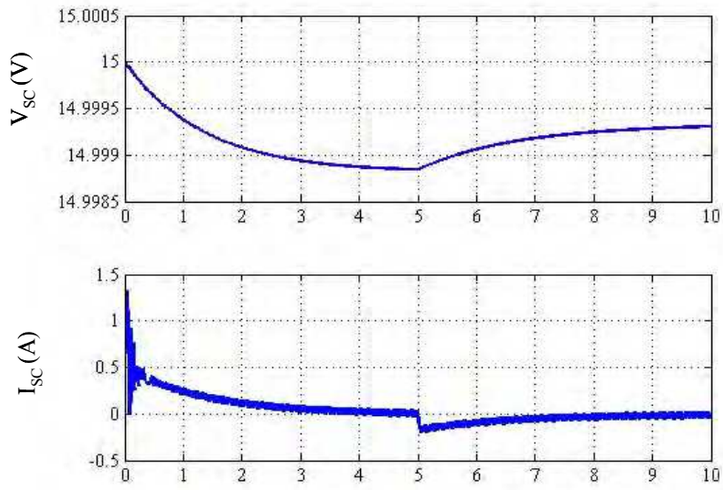

Fig. 19. SC voltage and SC current

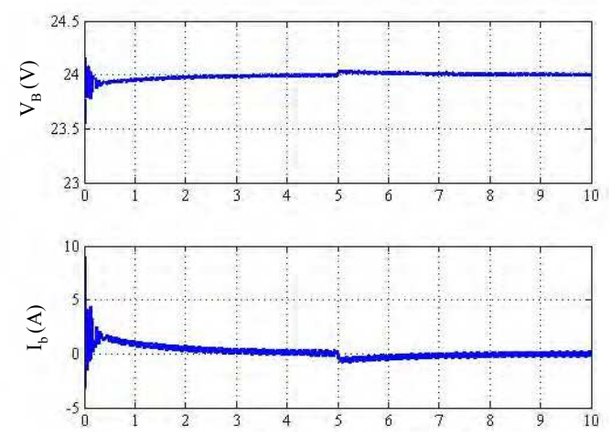

Fig. 20. Batteries voltage and batteries current

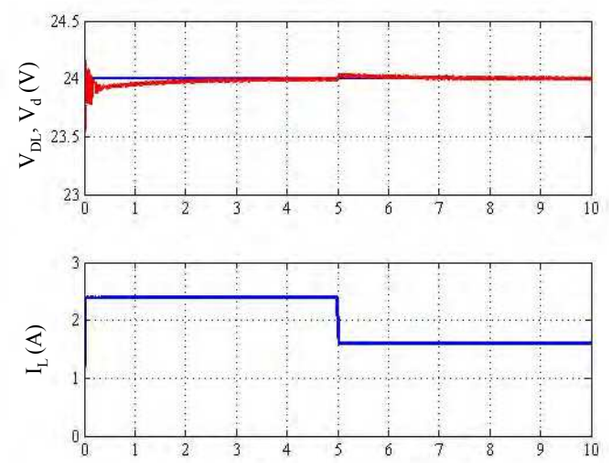

Fig.21. DC link voltage and load current

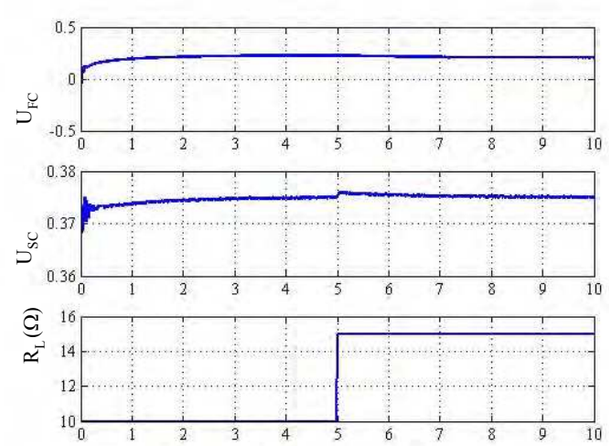

Fig. 22. (a) FC Boost control. (b) SC DC-DC (c) Load resistance change

4. Conclusion

In this paper, control principles of a hybrid DC source have been presented. This source uses the fuel cell as mean power source, SCs as auxiliary transient power source and batteries on the DC link.

Passivity Based Control and Sliding Mode Control principles have been applied and validated by simulation results. Include main findings and highlight the positive points of the simulation results and the possibility of applying this new concept in Fuel Cell applications.

PCH structure of the overall system is given exhibiting important physical properties in terms of variable interconnection and damping of the system. The problem of the DC Bus Voltage control is solved using simple linear controllers based on an IDA-PBC approach.

With the sliding mode principle control, we have a robustness control. But the sliding surface is generated in function of multiple variables: DC link voltage, SCs current and voltage.

With PBC, only two measures are needed to achieve the control aims of this complex system (the FC Voltage and the SC current), while for the Sliding mode control we need to achieve the control aims of this complex system (the FC Voltage, the SC current, the SC voltage, load and DC link currents). The sliding mode is faster in terms of response to a set point change or disruption.

The PBC control laws are completely independent from the system's parameters, and then this controller is robust towards the parameter variation. The Sliding mode controller is function of the system parameter and is therefore sensitive to there changes.

The PBC control laws are very simple to realize and produce continuous behavior while the sliding mode control is more complicated (realization of the surface and the control laws) and introduce nonlinearities by commutation.

Global Stability proofs are given and encouraging simulation results has been obtained.

Many benefits can be expected from the proposed structure such that supplying and absorbing the power picks by using SC which also allows recovering energy.

5. References

Kishinevsky, Y. & Zelingher, S. (2003). Coming clean with fuel cells, IEEE Power & Energy Magazine, vol. 1, issue: 6, Nov.-Dec. 2003, pp. 20-25.

Larminie, J. & Dicks, A. (2000). Fuel cell systems explained, Wiley, 2000.

Pischinger, S.; Schönfelder, C. & Ogrzewalla, J. (2006). Analysis of dynamic requirements for fuel cell systems for vehicle applications, J. Power Sources, vol. 154, no. 2, pp. 420-427, March 2006.

Moore, R. M.; Hauer, K. H.; Ramaswamy, S. & Cunningham, J. M. (2006). Energy utilization and efficiency analysis for hydrogen fuel cell vehicles, J. Power Sources, 2006.

Corbo, P.; Corcione, F. E.; Migliardini, F. & Veneri, O. (2006). Experimental assessment of energy-management strategies in fuel-cell propulsion systems, J. Power Sources, 2006.

Rufer, A.; Hotellier, D. & Barrade, P. (2004). A Supercapacitor-Based Energy-Storage Substation for Voltage - Compensation in Weak Transportation Networks," IEEE Trans. Power Delivery, vol. 19, no. 2, April 2004, pp. 629-636.

Thounthong, P.; Raël, S. & Davat, B. (2007). A new control strategy of fuel cell and supercapacitors association for distributed generation system, IEEE Trans. Ind. Electron, Volume 54, Issue 6, Dec. 2007 Page(s): 3225 – 3233

Corrêa, J. M.; Farret, F. A.; Gomes, J. R. & Simões, M. G. (2003). Simulation of fuel-cell stacks using a computer-controlled power rectifier with the purposes of actual high-power injection applications, IEEE Trans. Ind. App., vol. 39, no. 4, pp. 1136-1142, July/Aug. 2003.

Benziger, J. B.; Satterfield, M. B.; Hogarth, W. H. J.; Nehlsen, J. P. & Kevrekidis; I. G. (2006). The power performance curve for engineering analysis of fuel cells, J. Power Sources, 2006.

Granovskii, M.; Dincer, I. & Rosen, M. A. (2006). Environmental and economic aspects of hydrogen production and utilization in fuel cell vehicles, J. Power Sources, vol. 157, pp. 411-421, June 19, 2006

Ortega, R.; van der Schaft, A.J.; Maschke, B. & Escobar, G. (2002). Interconnection and damping assignment passivity–based control of port–controlled hamiltonian systems, Automatica, vol.38(4), pp.585–596, 2002.

Becherif, M. & Mendes, E. (2006). Stability and robustness of Disturbed- Port Controlled Hamiltonian system with Dissipation, 16th IFAC World Congress, Prague, 2005.

Becherif, M. & Ayad, M. Y. (2006). Modelling and Passivity-Based Control of Hybrid Sources: Fuel cell and Supercapacitors, *In* 41st IEEE-IAS 2006, USA.

Ayad, M. Y.; Gualous, A.; Cirrincione, M. & Miraoui, A. (2007). Study And Realization Of A Power Source Using Supercapacitors Matrix and Fuel cell, in Proc. 2nd European Ele-Drive Transportation Conference EET-2007 - Brussels, 30th May - 1st June 2007

Ayad, M. Y.; Pierfederici, S.; Raël, S. & Davat, B. (2007). Voltage Regulated Hybrid DC Source using supercapacitors, Energy Conversion and Management, Volume 48, Issue 7, July 2007, Pages 2196-2202.

Belhachemi, F.; Rael, S. & Davat, B. (2000). A Physical based model of power elctric double layer supercapacitors, IAS 2000, 35th IEEE Industry Applications Conference, Rome, 8-12 October

Rao, V.; Singhal, G.; Kumar, A. & Navet, N. (2005). Model for Embedded Systems Battery, Proceedings of the 18th International Conference on VLSI Design held jointly with 4th International Conference on Embedded Systems Design (IEEE-VLSID'05), 2005.

Chen, M.; Gabriel, A.; Rincon-Mora. (2006). Accurate Electrical Battery Model Capable of Predicting Runtime and *I–V* Performance. . *IEEE Trans. Energy Convers*, Vol. 21, No.2, pp.504-511 June 2006.

Salameh, Z.M.; Casacca, M.A. & Lynch, W.A. (1992). A mathematical model for lead-acid batteries, *IEEE Trans. Energy Convers.*, vol. 7, no. 1, pp. 93–98, Mar. 1992.

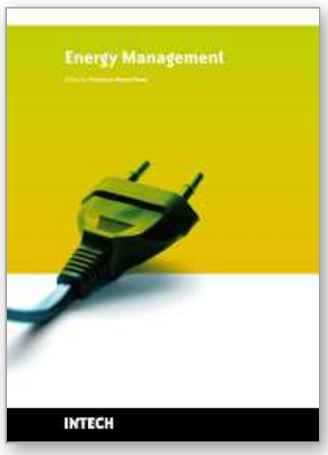

Energy Management

Edited by Francisco Macia Perez

ISBN 978-953-307-065-0

Hard cover, 246 pages

Publisher InTech

Published online 01, March, 2010

Published in print edition March, 2010

Forecasts point to a huge increase in energy demand over the next 25 years, with a direct and immediate impact on the exhaustion of fossil fuels, the increase in pollution levels and the global warming that will have significant consequences for all sectors of society. Irrespective of the likelihood of these predictions or what researchers in different scientific disciplines may believe or publicly say about how critical the energy situation may be on a world level, it is without doubt one of the great debates that has stirred up public interest in modern times. We should probably already be thinking about the design of a worldwide strategic plan for energy management across the planet. It would include measures to raise awareness, educate the different actors involved, develop policies, provide resources, prioritise actions and establish contingency plans. This process is complex and depends on political, social, economic and technological factors that are hard to take into account simultaneously. Then, before such a plan is formulated, studies such as those described in this book can serve to illustrate what Information and Communication Technologies have to offer in this sphere and, with luck, to create a reference to encourage investigators in the pursuit of new and better solutions.

InTech Europe

University Campus STeP Ri
Slavka Krautzeka 83/A
51000 Rijeka, Croatia
Phone: +385 (51) 770 447
Fax: +385 (51) 686 166
www.intechopen.com

InTech China

Unit 405, Office Block, Hotel Equatorial Shanghai
No.65, Yan An Road (West), Shanghai, 200040, China
中国上海市延安西路65号上海国际贵都大饭店办公楼405单元
Phone: +86-21-62489820
Fax: +86-21-62489821

IntechOpen